atmosphere

MDPI

Article

Apportionment of Vehicle Fleet Emissions by Linear Regression, Positive Matrix Factorization, and Emission Modeling

Xiaoliang Wang [1,*], L.-W. Antony Chen [2], Minggen Lu [3], Kin-Fai Ho [4], Shun-Cheng Lee [5], Steven Sai Hang Ho [1,6], Judith C. Chow [1] and John G. Watson [1]

1 Division of Atmospheric Sciences, Desert Research Institute, Reno, NV 89512, USA; stevenho@hkpsrl.org (S.S.H.H.); judy.chow@dri.edu (J.C.C.); john.watson@dri.edu (J.G.W.)
2 Department of Environmental and Occupational Health, University of Nevada-Las Vegas, Las Vegas, NV 89154, USA; lung-wen.chen@unlv.edu
3 School of Public Health, University of Nevada-Reno, Reno, NV 89557, USA; minggenl@unr.edu
4 The Jockey Club School of Public Health and Primary Care, The Chinese University of Hong Kong, Hong Kong, China; kfho@cuhk.edu.hk
5 Department of Civil and Environmental Engineering, Hong Kong Polytechnic University, Hong Kong, China; shun-cheng.lee@polyu.edu.hk
6 Hong Kong Premium Services and Research Laboratory, Hong Kong, China
* Correspondence: xiaoliang.wang@dri.edu; Tel.: +1-775-674-7177

Abstract: Real-world emission factors for different vehicle types and their contributions to roadside air pollution are needed for air-quality management. Tunnel measurements have been used to estimate emission factors for several vehicle types using linear regression or receptor-based source apportionment. However, the accuracy and uncertainties of these methods have not been sufficiently discussed. This study applies four methods to derive emission factors for different vehicle types from tunnel measurements in Hong Kong, China: (1) simple linear regressions (SLR); (2) multiple linear regressions (MLR); (3) positive matrix factorization (PMF); and (4) EMission FACtors for Hong Kong (EMFAC-HK). Separable vehicle types include those fueled by liquefied petroleum gas (LPG), gasoline, and diesel. PMF was the most useful, as it simultaneously seeks source profiles and source contributions. Diesel-, gasoline-, and LPG-fueled vehicle emissions accounted for 52%, 10%, and 5% of $PM_{2.5}$ mass, respectively, while ammonium sulfate (~20%), ammonium nitrate (6%), and road dust (7%) were also large contributors. MLR exhibited the highest relative uncertainties, typically over twice those determined by SLR. EMFAC-HK has the lowest relative uncertainties due to its assumption of a single average emission factor for each pollutant and each vehicle category under specific conditions. The relative uncertainties of SLR and PMF are comparable.

Keywords: tunnel; $PM_{2.5}$; source apportionment; PMF; HERM; linear regression; EMFAC; vehicle emission; emission factor; source profile; air quality

Citation: Wang, X.; Chen, L.-W.A.; Lu, M.; Ho, K.-F.; Lee, S.-C.; Ho, S.S.H.; Chow, J.C.; Watson, J.G. Apportionment of Vehicle Fleet Emissions by Linear Regression, Positive Matrix Factorization, and Emission Modeling. *Atmosphere* **2022**, *13*, 1066. https://doi.org/10.3390/atmos13071066

Academic Editor: Kenichi Tonokura

Received: 15 June 2022
Accepted: 4 July 2022
Published: 6 July 2022

1. Introduction

On-road vehicle emissions are targeted for reductions due to their large contributions to greenhouse gases and air pollutants, including carbon dioxide (CO_2), carbon monoxide (CO), volatile organic compounds (VOC), nitrogen oxides (NO_x), particulate matter (PM), and other air toxics. Accurate emission factors (EFs), which describe the emitted pollutant mass (g) per distance driven (km) or amount of fuel consumed (kg) for different vehicle categories are needed for emission inventories, emission standards enforcement, and assessments of air quality and health effects.

EFs can be obtained from laboratory dynamometer testing, on-road or roadside plume identification, onboard measurements, remote sensing, and tunnel studies [1–3]. Among these methods, tunnel studies have the advantage of being able to sample many vehicles representative of local real-world fuel and fleet compositions under in-use conditions [4,5].

In-tunnel concentrations are dominated by traffic emissions, and the influence of background and other pollution sources can be determined by measurements at tunnel inlet and outlet locations.

Linear regression methods, as first introduced by Pierson et al. [6], have been used to apportion the measured fleet-average EFs to different vehicle fleets, typically gasoline and diesel vehicles (GV and DV, respectively) or light and heavy-duty vehicles (LD and HD, respectively). For example, when the measured EF is regressed against the DV fraction (f_{DV}), the intercept of the regression line with the vertical axis at f_{DV} = 0 is the EF for GV, while the intercept at f_{DV} = 100% is the EF for DV. Pierson et al. (1996) cautioned that single values of EFs for the two regressed vehicle categories are not exact, due to large vehicle-to-vehicle emission variabilities within the same category. The linear regression method can be extended to include other factors affecting EFs. Colberg et al. [7] studied the effects of weekday and weekend differences as well as vehicle speed. The main challenge for tunnel data analysis with linear regression is that many tunnels have a limited range of DV or HD fractions (typically < 50%), which results in large uncertainties when extrapolating EFs from the narrow range of measured f_{HD} fractions to the f_{HD} of 0% and 100% end points [8]. For example, Song et al. [9] derived heavy-duty diesel vehicle (HDDV) EFs by extrapolating from measured data with f_{HDDV} < 10% to EFs at f_{HDDV} = 100%. To reduce these uncertainties, several studies used tunnels where LD and HD vehicles were separated into different bores. The Fort McHenry tunnel studied by Pierson et al. [6] had f_{HD} of 0.2–4.0% in one bore and 4.4–72.5% in the other bore. For tunnels without vehicle separations, studies have sampled during different hours of the day to obtain larger f_{HD} or f_{DV} ranges. Decreasing sample durations (e.g., 1-h instead of 24-h averages) can also increase the fleet composition variability [8,9]. The large vehicle-to-vehicle emission variability and limited f_{HD} or f_{DV} ranges in tunnels are the main sources of uncertainty in emissions apportionment performed using the linear regression method.

More advanced receptor-based source apportionment methods seek solutions to the chemical-mass balance equations (CMB) [10]. Commonly used approaches include the effective variance solution (EV-CMB) [11] and multivariate factor analysis solutions, such as principal component analysis (PCA) [12] and positive matrix factorization (PMF) [13]. These solutions use the entire pattern of source and receptor measurements to obtain more source specificity and reduce uncertainty. As long as the number of source types is less than or equal to the number of measured properties, the EV-CMB can be solved for individual samples. However, the solution depends on measured source profiles that represent emissions from the different vehicle types [14,15]. One of the challenges for EV-CMB is that existing source profiles are often dated and do not contain modern markers or represent the specific sources in the study area. This is also true for vehicle emission profiles as advances in fuels, engine designs, and emission control technologies have caused continuous changes in source profiles [16]. Therefore, only a few studies applied EV-CMB to identify and quantify traffic-generated source contributions [17–19]. Other studies used factor analysis [20,21], such as the PCA or PMF solutions. The factor solutions also require measured source profiles to associate the factor with a source type, although the derived ratios among the marker species may differ. It is often the case, however, that the derived factors exhibit mixed profiles, as the different species concentrations tend to be highly correlated, thereby resulting in uncertainties associated with factor identification. The factor models are most accurate when datasets are large, exhibit large ranges of variability among the measured components, and have low correlations among the markers for different source types. PCA coupled with multiple linear regression analysis (MLRA) was applied in several studies to apportion traffic emissions [22,23]. PCA may lead to less adequate factor resolution and less plausible results than PMF [21,22]. Due to the uncertainties in source apportionment approaches, a "weight of evidence" approach is recommended to use additional available information (e.g., local emission inventories, source profiles, and modeling performance measures), apply several receptor-modeling

techniques, and reconcile receptor-oriented and source-oriented models to evaluate the uncertainties and increase the degree of confidence [10,14,24].

Vehicle emission models are used to assess mobile source emissions and compile emission inventories [25]. These models typically use baseline EFs with several adjustment factors such as vehicle age, speed, and ambient temperature, which are typically derived from emission standards, laboratory testing, and real-world measurement. Comparing emission models with tunnel measurements enables the assessment of model performance by reconciling the differences between the source and receptor sides [1,26]. The detailed estimates of emissions by vehicle classes and fuels in emission models also offer guidance on emission control priorities [27].

While many tunnel studies attempt to apportion the measured fleet EFs to different vehicle types, few studies have compared the results from the apportionment methods. The main objectives of this study are to: (1) compare fuel-specific fleet EFs estimated by linear regressions, PMF, and emission modeling; (2) quantify emission contributions from different fleet components; and (3) evaluate PMF source profiles. Data from the Shing Mun Tunnel (SMT) in Hong Kong is used as a case study [28,29].

2. Methods

2.1. Vehicle Emission Measurements in the Shing Mun Tunnel

The SMT is a two-bore highway tunnel on the Hong Kong Route 9 expressway. Each bore has a cross-sectional area of 70 m^2 with two traffic lanes traveling in the same direction. Vehicle emissions were measured in the east section of the south bore, which has a total length of 1.6 km with an uphill grade of 1.054% from the entrance to the exit. The tunnel has a daily vehicle flow of ~53,000 in both directions, with an average liquefied petroleum gas (LPG), gasoline, and diesel fleet mix of 13%, 45%, and 42% [28]. As the closest highway ramp is ~2.5 km from the tunnel entrance, most vehicles are likely in hot-stabilized operating conditions, driving near the posted speed limit of 80 km h^{-1}.

Vehicle emission measurements were conducted in the SMT from January to March 2015, with experimental details described in previous publications [28–30]. The sampling configuration is illustrated in Figure S1 [28]. Briefly, measurements were carried out simultaneously at inlet and outlet sites separated by 600 m. Due to access and power constraints, the inlet sampling site was 686 m from the tunnel entrance, while the outlet sampling site was 350 m before the tunnel exit. Concentrations of CO, CO_2, nitric oxide (NO), nitrogen dioxide (NO_2), and $PM_{2.5}$ (by light scattering) were measured with near real-time instruments at time resolutions of 1 s to 1 min. Wind speed, wind direction, barometric pressure (P), temperature (T), and relative humidity (RH) were monitored by weather stations every five minutes. Traffic flow was recorded by two video cameras. Non-methane hydrocarbons (NMHC) were collected in pre-cleaned and pre-evacuated 2 L stainless-steel canisters with a flow rate of 27.3 mL min^{-1} using a multi-port canister sampler. $PM_{2.5}$ samples were simultaneously collected on one Teflon-membrane filter and two quartz-fiber filters at a flowrate of 37.7 L min^{-1} each. While real-time gas and PM monitors, weather stations, and video cameras were operated continuously, integrated samples were collected over 2 h sampling periods, which covered morning and evening rush hours (i.e., 0800–1000 and 1700–1900 local standard time [LST]) as well as midday hours (i.e., 1100–1300 and 1400–1600 LST).

Canister samples were analyzed for 66 speciated NMHC (C2–C12) using gas chromatography/mass spectrometry (GC/MS) following the U.S. EPA Method TO-15 [30,31]. $PM_{2.5}$ filter samples were analyzed for mass, elements, ions, carbon fractions, and organic compounds [28]. Teflon-membrane filters were analyzed for mass by gravimetry [32] and 51 elements (sodium through uranium) by X-ray fluorescence (XRF) [33]. Half of the quartz-fiber filters were extracted in distilled deionized water and analyzed for six water-soluble ions, including chloride (Cl^-), nitrate (NO_3^-), sulfate (SO_4^{2-}), ammonium (NH_4^+), sodium (Na^+), and potassium (K^+), using ion chromatography (IC) [34]. Organic carbon (OC), elemental carbon (EC), and eight thermal fractions (OC1–OC4, pyrolyzed carbon [OP],

EC1–EC3) were quantified by the IMPROVE_A thermal/optical protocol [35] from a punch of the quartz-fiber filter. Another 2–3 punches of the quartz-fiber filter were analyzed for 113 non-polar organic compounds including alkanes, alkenes, hopanes, steranes, and PAHs by thermal desorption (TD)-GC/MS [36–38]. The backup citric-acid-impregnated cellulose-fiber filter was analyzed for NH_3 as NH_4^+ by IC, and the backup quartz-fiber filter was analyzed by the IMPROVE_A protocol to estimate the organic vapors adsorbed onto the front quartz-fiber filter [39].

The distance-based emission factor (EF_D; in g veh^{-1} km^{-1}) calculation uses the mass balance principle, i.e., the mass of pollutant i produced by vehicles in the tunnel section bounded by the inlet and outlet sites during a sampling period Δt is the difference between the mass leaving the outlet site and that entering the inlet site [6]:

$$EF_D = \frac{(C_{i,out}U_{out} - C_{i,in}U_{in})A\Delta t}{N \times L}, \quad (1)$$

where C_i (g m^{-3}) is the average concentration of the pollutant i, U (m s^{-1}) is the wind speed, the subscripts in and out denote the values measured at the inlet and outlet sampling sites, respectively, A (m^2) is the tunnel cross-sectional area (70 m^2 for SMT); Δt (s) is the sampling period, N is the number of vehicles passing through the tunnel section during Δt, and L (m) is the length of the tunnel section between the inlet and outlet sampling sites (0.6 km in this study).

The traffic videos taken from the tunnel entrance were used to manually classify the fleet into nine categories (i.e., motorcycle, private car, taxi, light goods vehicle, medium goods vehicle, heavy goods vehicle, light bus, single deck bus, and double-decker bus) with a time resolution of 15 min for each of the 2 h sampling period. The total vehicle numbers from manual counting differed by <4% from those recorded hourly by the SMT toll booths. The allocation of the fleet to LPG, GV, and DV was based on vehicle kilometers traveled (VKT) by different vehicle classes classified by Emission FACtors for Hong Kong (EMFAC-HK) [27].

2.2. Emission Apportionment by Linear Regressions

Linear regressions have been used in tunnel studies to apportion emissions to different fleet components using the following equation [6,40]:

$$EF_i = \sum_m (EF_{i,m} \times f_m) + \varepsilon_i, \quad (2)$$

where $EF_{i,m}$ is the EF of pollutant i by the m^{th} fleet component, f_m is the percentage of the m^{th} vehicle fleet component, and ε_i is the error term. Most previous tunnel studies used simple linear regressions (SLR) to separate the fleet into two components (i.e., m = 2): LD and HD or non-diesel vehicles (NDV) and DV. An example of SLR is shown in Figure 1. The fleet-average EF of NO_x is plotted against the percentage of DV (f_{DV}). The intercepts of the regression line at 0% and 100% DV are the EFs for NDV and DV, respectively. Due to the fact that the fleet in the SMT consists of LPG, GV, and DV, multiple linear regressions (MLR) with m = 3 were also conducted to apportion EFs to these three fleet components. Th predicted values are reported using 95% confidence intervals to represent uncertainties. The estimates are statistically different from zero if the corresponding confidence intervals do not cover zero.

Outliers can distort the representativeness of regression analysis results [8,22]. The median absolute deviation (MAD) method is applied to remove outliers [41]. Specifically, the absolute value of the difference between each observed value and the median of the data is calculated to generate a new median of the differences, which is multiplied by an empirical constant to yield the MAD. An observed value is classified as an outlier if it exceeds three times the MAD value.

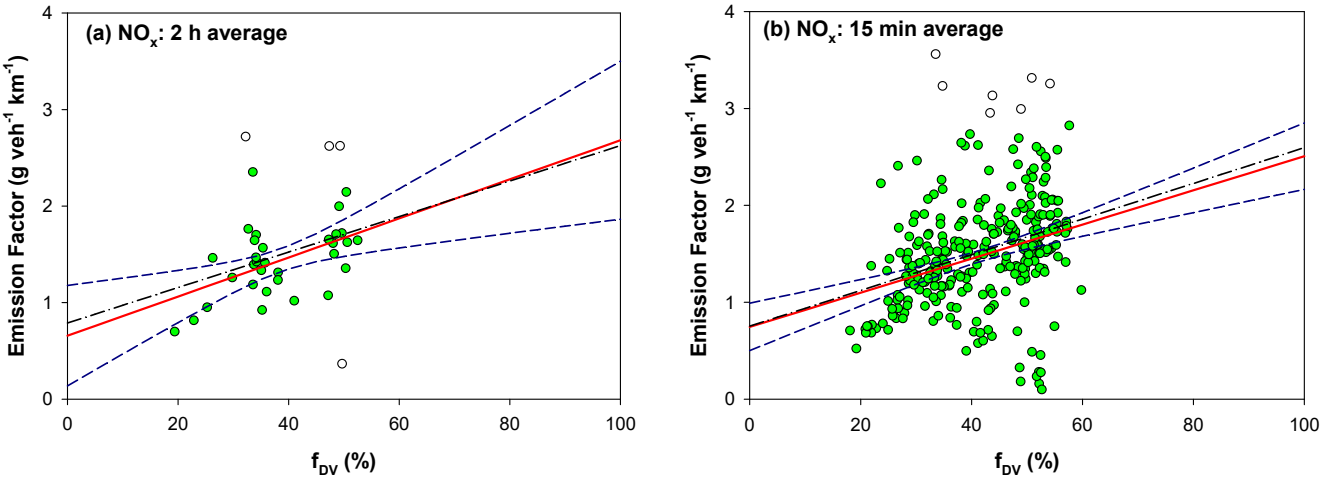

Figure 1. Comparison of simple linear regression of NO_x emission factor vs. diesel vehicle fraction for data averaged over (**a**) 2 h and (**b**) 15 min. The black dash-dotted line shows non-robust regression over all data points. The red solid line shows robust regression excluding the outlier (unfilled symbols) data points. The blue dashed lines indicate 95% coincidence intervals for the robust regression.

The linear regression method assumes that emissions from different vehicle categories are linearly dependent on the vehicle number fraction for each category. Since vehicles under the same category may have different EFs (e.g., gasoline-fueled motorcycles and passenger cars), the vehicle number fraction may not be an accurate indicator for emissions. Furthermore, other emission sources, such as non-tailpipe emissions, will also affect measured pollutant concentrations. A more appropriate method to apportion emissions to different fleet components could be receptor-based source apportionment.

2.3. Vehicle Source Apportionment by PMF

The CMB equations link source profiles and source contributions to ambient chemical concentrations:

$$C_{i,t} = \sum_j F_{i,j} S_{j,t} + \varepsilon_{i,t}, \quad (3)$$

where $C_{i,t}$ is the measured concentration of species i at time t, $F_{i,j}$ is the fraction of species i in source profile j, and $S_{j,t}$ is the source contribution estimate (SCE) of source j at time t. $\varepsilon_{i,t}$ is the deviation between the modeled and measured concentrations due to random variability, which is the term that is minimized in the PMF calculation. PMF solves $F_{i,j}$ and $S_{j,t}$ simultaneously by minimizing the Q value as below:

$$Q = \sum_t \sum_i {q_{i,t}}^2 = \sum_t \sum_i \frac{\left(C_{i,t} - \sum_j F_{i,j} S_{j,t}\right)^2}{{\Delta C_{i,t}}^2}, \quad (4)$$

where $\Delta C_{i,t}$ is the weighting factor for $C_{i,t}$, which mainly corresponds to the random and/or systematic measurement uncertainties. The number of source factors in the model is pre-specified, usually based on a sensitivity test [42].

The tunnel study acquired 132 ambient $PM_{2.5}$ samples (from both inlet and outlet sites) characterized for over 200 inorganic and organic species. Among these, 61 samples also had concurrent NMHC measurements. To ensure that all measured species are used in the model while the missing values are heavily down-weighted in the fitting process, all missing data were replaced with the average concentrations throughout the study period, with uncertainties of 100 times the respective concentrations [43]. Sensitivity tests showed that varying the uncertainties from 10 to 100 times the average values did not change the SCEs and profiles appreciably. Additionally, $PM_{2.5}$ and NMHC species, CO_2, CO, NO,

NO_2, NO_x, and SO_2 were averaged into two-hour intervals and included in the receptor model.

Major sources contributing to SMT samples include: (1) vehicle (LPG, GV, and DV) exhaust, (2) resuspended road dust and non-tailpipe emissions, and (3) background air. The background air in Hong Kong, especially around the SMT, was dominated by motor vehicle exhausts and secondary sulfate and/or nitrate [44]. Conceptually, at least six sources of $PM_{2.5}$ and NMHC are required for the SMT source apportionment, namely diesel (exhaust), gasoline (exhaust), LPG (exhaust), (road) dust, secondary ammonium sulfate ($(NH_4)_2SO_4$), and secondary ammonium nitrate (NH_4NO_3). Profiles for secondary $(NH_4)_2SO_4$ and NH_4NO_3 should only contain secondary species, as the primary species should be incorporated into primary source profiles [45,46]. Road dust samples in the tunnel were collected and analyzed for the same species as the ambient $PM_{2.5}$ samples to construct a "dust" source profile, which further constrained the PM factors. Source profiles for LPG, GV, and DV exhaust specific to Hong Kong with all the markers acquired in this study were not available, though previous studies have identified important marker compounds in these emissions.

The PMF calculation was carried out using the Hybrid Environmental Receptor Model (HERM), which allows specifying known source profiles as constraints on the PMF solutions [47–49]. In the HERM formulation, the weighting factor $\Delta C_{i,t}{}^2$ is replaced with $EV_{i,t}$ that takes into account uncertainties of both measured pollutant concentrations ($\Delta C_{i,t}$) and profile abundances ($\Delta F_{i,j}$):

$$EV_{i,t} = \Delta C_{i,t}{}^2 + \sum_j (\Delta F_{i,j}{}^2 S_{j,t}{}^2 + \delta_{i,j} \Delta C_{i,t}{}^2), \quad (5)$$

where $\delta_{i,j} = 0$ if the source profile element $F_{i,j}$ is specified, and $\delta_{i,j} = 1$ when $F_{i,j}$ is to be solved. Three- to nine-factor solutions were explored, with the first three factors constrained by the secondary $(NH_4)_2SO_4$, secondary NH_4NO_3, and dust source profiles. The fractional change of Q value (ΔQ_m) from the m to m + 1 factor solutions was calculated, and this showed little change after m = 6 (Figure S2). This is consistent with a six-factor solution being appropriate for the dataset; any additional source types would be minor contributors.

The HERM-PMF results can be evaluated through performance measures, particularly the correlation between the measured and calculated concentrations ($r_i{}^2$) and the scaled residuals ($\chi_i{}^2$). HERM calculates $r_i{}^2$ and $\chi_i{}^2$ by the following equations:

$$r_i{}^2 = 1 - \frac{\left(K(I-J) - \sum_i \sum_j \delta_{i,j}\right)\chi_i{}^2}{I \times \left(\sum_t \frac{C_{i,t}{}^2}{EV_{i,t}}\right)}, \quad (6)$$

$$\chi_i{}^2 = \frac{I}{K(I-J) - \sum_i \sum_j \delta_{i,j}} \sum_t \frac{\left(C_{i,t} - \sum_j F_{i,j} S_{j,t}\right)^2}{EV_{i,t}}, \quad (7)$$

where I, J, and K are the total number of species, factors, and samples, respectively [47]. High correlation coefficients and/or low residuals indicate a good fit. As shown in Figure S3, the six-factor solution explained the majority of $PM_{2.5}$ inorganic components with $r_i{}^2 > 0.9$, including OC, EC, S, $NO_3{}^-$, $NH_4{}^+$, and key mineral elements (e.g., Si, Fe, and K). Some of these species showed $\chi_i{}^2$ values greater than 1, and thus dominated the Q value (and PMF solution) due to higher measurement precisions. Organic markers did not fit well with $r_i{}^2 < 0.9$, though their $\chi_i{}^2$ values were generally low (<1). This is consistent with a lower signal-to-noise ratio for these organic markers. Species such as vanadium (V), nickel (Ni), chloride (Cl^-), and acenaphthylene (ACNAPY) showed poor fits (low correlations and larger scaled residuals) implying potential impacts from additional sources (e.g., crude oil/coal combustion and sea salt) [50]. As noted, contributions from these sources to tunnel $PM_{2.5}$ were too small to be quantified by PMF even if the number of factors was increased to

7 or 8 and/or after factor rotations. They are not expected to bias the SCEs for major sources (i.e., mobile exhausts and road dust) as they are minor components in these emissions.

The PMF performance for NMHCs and gases is shown in Figure S4. Most species showed χ_i^2 values between 0.1 and 10, indicating that the Q values were more evenly distributed among all species, possibly due to a more uniform estimate of measurement uncertainty. Species that were reproduced well by the HERM-PMF solution include markers for LPG exhaust: isobutane, propane, and n-butane ($r_i^2 > 0.95$), as well as propene ($r_i^2 = 0.98$), a marker for diesel exhaust [51]. The model also fitted NO, NO_2, and NO_x ($r_i^2 = 0.93$–0.95) better than CO ($r_i^2 = 0.79$). Isoprene and α-pinene, markers for biogenic emissions, were not well-explained by the PMF solution; they were small portions of the total NMHCs in the tunnel. Ethylbenzene, mp-xylene, and o-xylene had high scaled residuals, mainly because a few outliers were found at the outlet sampling site on two sampled days. The extreme concentrations (>10 times the average) of these outliers may result from unknown contamination, as they only appeared at the outlet sampling site. These outliers were weighted much less in the PMF due to the robust fitting algorithm [52].

The differences between outlet and inlet concentrations for each pollutant were used to calculate the fleet-average EF_{Fleet} using Equation (1). Due to the fact that the chemical speciation of $PM_{2.5}$ and NMHCs were conducted for 2 h integrated samples, EF_{Fleet} were calculated for each of the valid 2 h integrated samples. Diesel-vehicle specific EFs were then calculated using the equation below:

$$EF_{DV} = (FSC_{DV} \times EF_{Fleet})/f_{DV}, \quad (8)$$

where FSC_{DV} is the fractional DV contribution to the pollutant (e.g., $PM_{2.5}$), determined from the PMF source apportionment, and f_{DV} is the fraction of DV in the fleet. Secondary $(NH_4)_2SO_4$, secondary NH_4NO_3, and road dust did not contribute to EFs appreciably, as evidenced by similar concentrations between the outlet and inlet measurements [28]. Therefore, FSC_{DV} is defined as:

$$FSC_{DV} = SCE_{DV}/(SCE_{LPG} + SCE_{GV} + SCE_{DV}). \quad (9)$$

Equations (8) and (9) were also applied to LPG and GV as well as NDV (sum of LPG and GV) to determine EF_{LPG}, EF_{GV}, and EF_{NDV}. Since the EFs were determined for each 2 h sample, the average EFs and 95% confidence intervals of the means are reported as the final EFs and uncertainties for the LPG, GV, and DV.

2.4. Vehicle Emission Estimates by EMFAC-HK

EMFAC-HK is the vehicle emission model used to develop the official Hong Kong-wide vehicle emission inventories, and the "Emfac" mode of the EMFAC-HK V4.2 was used to model tunnel vehicle emissions in this study [27]. The model generates a matrix of EFs at a range of temperatures (0–40 °C), RH (0–100%), and vehicle speeds (0–130 km h^{-1}) for each vehicle class–fuel combination. Running exhaust EFs (in g veh^{-1} km^{-1}), i.e., emissions from the vehicle tailpipe while it is traveling on the road, were calculated for methane (CH_4), total hydrocarbon (THC), CO, CO_2, NO_2, NO_x, $PM_{2.5}$, and PM_{10}. The EF for NO (as NO_2) was calculated by subtracting NO_2 EF from that of NO_x (as NO_2). Additionally, evaporative running-loss EFs during vehicle operation (in g veh^{-1} min^{-1}) were calculated for CH_4 and THC. Since the EMFAC-HK does not directly output NMHC emissions, running exhaust emissions of NMHC were calculated by subtracting CH_4 from THC emissions. These EFs were organized as lookup tables associated with the combinations of T, RH, and vehicle speed values.

Vehicle emissions between the SMT outlet and inlet for each 15 min vehicle counting period were calculated as follows:

$$\text{Emissions} = \text{Emission Factor} \times \text{Source Activity}. \quad (10)$$

EFs were determined from the lookup table assuming a constant vehicle speed of 80 km h^{-1} (speed limit) and average ambient T and RH over each period. For running exhaust emissions, the source activity is the VKT (i.e., the number of vehicles in each class multiplied by the 0.6 km distance between the inlet and outlet sites). For CH_4 and THC evaporative running losses, the source activity is the average transit time (0.45 min) through the tunnel section times the number of vehicles in each class. LPG, GV, and DV emissions were calculated by summing emissions from all vehicles powered by the respective fuels; and the EFs for the entire fleet, as well as for each fuel, were calculated by dividing the total emissions by tunnel VKT of the fleet or vehicles with each fuel, either for every 15 min vehicle counting period or every 2 h integrated sample collection period.

3. Results and Discussion

3.1. Pollutant Apportionment by Linear Regression

Linear regressions were first conducted with continuous measurement data averaged to a 2 h time resolution to match the collection periods of the integrated samples. A plot of NO_x EF vs. f_{DV} is shown in Figure 1a as an example. The data has only a moderate linear trend, with a correlation coefficient (r) of 0.50. A simple linear regression using Equation (2) results in NO_x EFs average ± expanded uncertainty at 95% confidence intervals values of 0.66 ± 0.52 g veh^{-1} km^{-1} for NDV and 2.68 ± 0.87 g veh^{-1} km^{-1} for DV obtained at f_{DV} = 0 and 100%, respectively. The relative uncertainties (expanded uncertainty divided by average) are 79% and 32% for NDV and DV, respectively. These uncertainties were significantly reduced to 33% and 14% when the concentrations were averaged over the 15 min traffic counting periods. As shown in Figure 1b, the ranges of NO_x EFs improved to 0.74 ± 0.24 g veh^{-1} km^{-1} and 2.51 ± 0.34 g veh^{-1} km^{-1} for NDV and DV, respectively. Regression analyses for all measured pollutants are presented in Figure S5. Two factors contributed to this uncertainty reduction: first, as the number of data points increased eight times, the standard errors of the estimators decreased; second, the shorter averaging time increased the differentiation of emissions among different vehicle types, causing less overlap of contributions from different vehicle types to each data point [21]. Therefore, all linear regressions used 15 min average data except NMHC, for which only 2 h integrated data were available.

Figure 1 also shows the effects of including or excluding outliers for the SLR solution. Based on the outlier criterion of 3 times the value of MAD away from the median of the data, four outliers were identified in Figure 1a. Including the outliers resulted in NO_x EFs of 0.79 ± 0.77 g veh^{-1} km^{-1} for NDV and 2.63 ± 1.17 g veh^{-1} km^{-1} for DV, 20% higher and 2% lower than EFs without including the outliers, respectively. Similarly, seven outliers were identified in Figure 1b. Including outliers resulted in NO_x EFs of 0.75 ± 0.27 g veh^{-1} km^{-1} for NDV and 2.60 ± 0.38 g veh^{-1} km^{-1} for DV, which are, respectively, 1% and 3.5% higher than the EFs without including the outliers. The differences in mean EFs by including or excluding the outliers were < ±20% for most species.

EFs by SLR and MLR are compared in Table 1 and Table S1. For average DV EFs, the estimates using both methods agreed within 3% for NO, NO_x, and SO_2. The mean EFs for $PM_{2.5}$ and NO_2 were statistically similar, although $PM_{2.5}$ was 11% lower (p = 0.61) while NO_2 was 23% higher (p = 0.16) by MLR. The EF for CO_2 was 24% lower by MLR than that by SLR, and the difference was statistically significant (p < 0.05). The largest difference was found for CO, with SLR and MLR giving 1.83 ± 0.23 and 0.20 ± 0.43 g veh^{-1} km^{-1}, respectively. As shown in Figure S5b, the CO linear regression line has a shallow slope, resulting in a poor separation of NDV from DV contributions. Due to the additional separation of the NDV emissions to LPG and GV in MLR, the EF uncertainties by MLR are approximately twice those from SLR, causing LPG and NDV EFs for all pollutants except CO_2 and CO to not be statistically different from zero. Further, the differences between SLR and MLR can be partially explained by how the apportionment was obtained: MLR is based on multiple linear regression, while the results of SLR are predicted values at 0% and 100% based on simple linear regression.

Table 1. Comparison of emission factors (EF_D; average ± expanded uncertainty at 95% confidence interval) for different fleet components from different methods.

Vehicle Category	Method [a]	EF_D (g/vehicle/km)							
		CO_2	**CO**	**NMHCs**	**NO**	**NO_2**	**NO_x (as NO_2)**	**SO_2**	**$PM_{2.5}$**
Fleet Average	EMFAC-HK	311.3 ± 1.9	1.29 ± 0.01	0.088 ± 0.001	0.743 ± 0.011	0.193 ± 0.003	1.333 ± 0.017	NA	0.024 ± 0.000
	Measurement	301.8 ± 12.4	1.80 ± 0.25	0.059 ± 0.004	0.869 ± 0.152	0.245 ± 0.045	1.577 ± 0.276	0.047 ± 0.004	0.025 ± 0.005
LPG	MLR	212.2 ± 109.9	1.81 ± 1.32	NA [b]	0.580 ± 1.110	−0.190 ± 0.390	−0.030 ± 1.570	0.010 ± 0.050	−0.080 ± 0.060
	PMF	240.1 ± 45.3	1.68 ± 0.53	0.150 ± 0.054	0.490 ± 0.208	0.107 ± 0.051	0.868 ± 0.373	0.009 ± 0.004	0.011 ± 0.003
	EMFAC-HK	222.2 ± 0.6	3.15 ± 0.03	0.123 ± 0.002	0.874 ± 0.006	0.019 ± 0.000	1.359 ± 0.009	NA	0.000
Gasoline (GV)	MLR	158.0 ± 31.2	1.26 ± 0.38	NA	0.400 ± 0.310	0.220 ± 0.110	0.850 ± 0.510	0.020 ± 0.010	0.010 ± 0.020
	PMF	144.6 ± 23.8	0.90 ± 0.52	0.035 ± 0.021	0.148 ± 0.096	0.020 ± 0.014	0.251 ± 0.163	0.021 ± 0.015	0.007 ± 0.002
	EMFAC-HK	177.2 ± 0.4	1.39 ± 0.01	0.107 ± 0.002	0.064 ± 0.001	0.005 ± 0.000	0.103 ± 0.001	NA	0.002 ± 0.000
Non-Diesel (NDV)	SLR	209.9 ± 14.0	2.14 ± 0.17	0.082 ± 0.037 [c]	0.445 ± 0.139	0.053 ± 0.051	0.745 ± 0.245	0.022 ± 0.006	0.008 ± 0.008
	MLR	170.3 ± 49.1	1.38 ± 0.59	NA	0.44 ± 0.49	0.13 ± 0.17	0.65 ± 0.75	0.02 ± 0.02	−0.01 ± 0.03
	PMF	167.3 ± 18.0	1.09 ± 0.49	0.062 ± 0.025	0.230 ± 0.107	0.041 ± 0.020	0.398 ± 0.186	0.018 ± 0.012	0.008 ± 0.002
	EMFAC-HK	187.3 ± 0.4	1.78 ± 0.01	0.110 ± 0.002	0.248 ± 0.003	0.008 ± 0.000	0.388 ± 0.005	NA	0.002 ± 0.000
Diesel (DV)	SLR	418.5 ± 19.7	1.83 ± 0.23	0.008 ± 0.056 [c]	1.343 ± 0.195	0.473 ± 0.071	2.507 ± 0.342	0.078 ± 0.009	0.056 ± 0.011
	MLR	319.4 ± 36.9	0.20 ± 0.43	NA	1.390 ± 0.360	0.580 ± 0.130	2.560 ± 0.600	0.080 ± 0.020	0.050 ± 0.020
	PMF	499.2 ± 28.1	0.29 ± 0.08	0.035 ± 0.014	1.227 ± 0.441	0.367 ± 0.143	2.255 ± 0.819	0.044 ± 0.016	0.043 ± 0.006
	EMFAC-HK	489.3 ± 1.8	0.61 ± 0.00	0.057 ± 0.000	1.446 ± 0.009	0.455 ± 0.003	2.672 ± 0.014	NA	0.057 ± 0.000

[a] EMFAC-HK: EMission FACtors mobile source emission model localized for Hong Kong; MLR: multiple linear regression; PMF: positive matrix factorization; SLR: simple linear regression. [b] NA: not available. [c] Linear regression for NMHC was obtained from 2 h average data.

3.2. Comparison of Emission Factors Using Linear Regression, PMF, and EMFAC-HK

The EFs obtained from SLR, MLR, PMF, and EMFAC for LPG, GV, NDV, and DV are summarized in Table 1 and compared in Figure S6. The relative uncertainties are listed in Table S2, and the Student's t-test *p*-values for paired comparison are listed in Table S3, with $p < 0.05$ indicating EFs being statistically different.

Among the different apportionment methods, EMFAC-HK has the lowest (<2%) relative uncertainties (Table S2). This low variation is because EMFAC-HK aggregates the vehicle fleet into 16 categories and assigns a single average EF value to each category under specific environmental and operating conditions. This process artificially reduces the EF variabilities among vehicles, e.g., between low and high emitters [27]. On the other hand, MLR has the highest relative uncertainties, with many values exceeding ±100%, causing LPG and NDV EFs for many pollutants to not be statistically different from zero (Table S1). The relative uncertainties of SLR and PMF are comparable for many EFs by DV and NDV.

The main challenge in the evaluation of different apportionment methods is that the true EFs are unknown; therefore, the accuracy of each method cannot be assessed. For CO_2, the fleet EF from tunnel measurement and EMFAC-HK estimate agreed within 3% [27]. The CO_2 EFs, by most apportionment methods and EMFAC-HK, were statistically similar. The exception was for DV; the CO_2 EFs by SLR and MLR were significantly lower than those by PMF and EMFAC-HK. In principle, EMFAC-HK estimates CO_2 EFs most accurately among all pollutants, as fuel efficiency is the only factor to be modeled. The agreement of EMFAC-HK and PMF CO_2 EFs adds credibility to the PMF apportionment, especially considering that the PMF method does not explicitly use vehicle fraction information. MLR reported lower CO_2 EFs than SLR for both DV and NDV, implying that biases caused by assuming the same EFs for GV and LPG in SLR could not be ignored.

For CO, MLR and PMF were statistically similar for all vehicle categories, while most other methods were different. SLR showed the highest EFs for DV and NDV, likely because of the shallow slope in the regression causing inaccurate apportionment to NDV and DV (Figure S5b). EMFAC-HK may not estimate CO emissions accurately as it reported a fleet-average EF for CO that is lower than the value measured in the tunnel by ~30% [27]. For NMHC, the fleet EF estimated by EMFAC-HK was ~50% higher than the measured value. Correspondingly, the EFs by EMFAC-HK were higher than those by PMF for all vehicle categories except LPG, for which they were comparable. SLR was applied to 2 h average data, resulting in larger uncertainties. For NO, NO_2, and NO_x, the EFs calculated by most methods were statistically similar for NDV and DV, likely due to their larger EF differences, as reflected by the higher slopes in Figure S5d–f. More variabilities are observed in the EFs for LPG and GV due to their lower EF values and higher uncertainties. For SO_2, PMF and MLR had an excellent agreement for LPG, GV, and NDV; similarly, SLR and MLR agree on NDV and DV. The only exception is that the SO_2 EF by PMF was about half of that by SLR and MLR for DV. For $PM_{2.5}$, emissions are dominated by DV, and the EFs for DV by different methods agree reasonably well (0.043–0.057 g veh^{-1} km^{-1}). For LPG, GV, and NDV, due to their lower emissions, the $PM_{2.5}$ EFs by SLR and MLR were not statistically different from zero; similarly, the EFs by EMFAC-HK were also low, because it assumes no PM emission from LPG vehicles. On the other hand, PMF reported $PM_{2.5}$ EF values of 0.011 ± 0.003, 0.007 ± 0.002, and 0.008 ± 0.002 g veh^{-1} km^{-1} for LPG, GV, and NDV, respectively, that differed significantly from zero.

3.3. Source Profiles and Source Contributions Derived by PMF

For NMHCs measured in the SMT, alkanes and cycloalkanes are the two most abundant groups (a sum of 59% of the total NMHCs mass concentration), followed by aromatics (23%), alkenes (14%), and alkynes (4%) [29,30]. Figure 2a shows the average abundance of NMHC species with abundances exceeding 0.5% of total NMHCs. Among the 66 quantified NMHCs, the ten most abundant species in a descending order were: n-butane (16.3 ± 4.9%), isobutane (11.9 ± 3.7%), propane (9.9 ± 2.1%), toluene, (9.2 ± 3.7%), ethene (7.4 ± 1.9%), m/p-xylene (5.5 ± 8.9%), isopentane (4.5 ± 1.1%), ethane (4.0 ± 1.2%), ethyne (4.0 ± 1.0%),

and propene (3.2 ± 0.8%). Among these species, n-butane, isobutane, and propane are major constituents of LPG; toluene, isopentane, and m/p-xylene are markers for gasoline fuel; and ethyne, ethene, and ethane are combustion products and markers for tailpipe emissions [51,53,54].

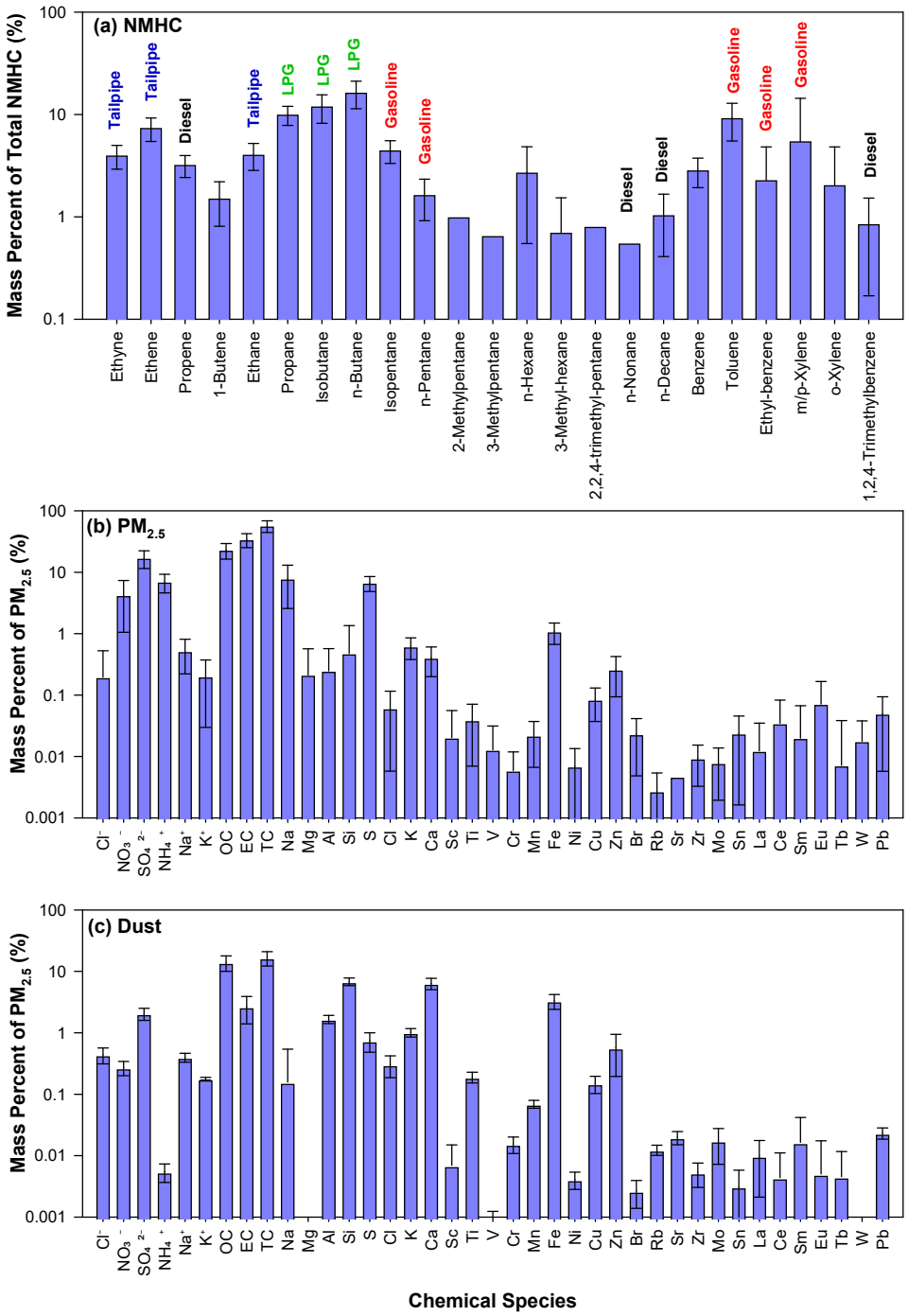

Figure 2. Average abundances (% of mass) for (**a**) NMHC species, (**b**) $PM_{2.5}$ components, and (**c**) resuspended dust components. Markers specific for diesel, gasoline, LPG, or tailpipe emissions are indicated in (**a**). Error bars indicate the standard deviations of multiple samples.

For the $PM_{2.5}$ samples, EC (33.8 ± 8.6%) and organic matter (OM; 27.5 ± 7.9%) are the most abundant constituents, followed by SO_4^{2-} (16.9 ± 5.4%), NH_4^+ (6.9 ± 2.3%), and geological materials (5.1 ± 3.3%). Figure 2b shows the $PM_{2.5}$ profile for ions, carbon, and elements. Additionally, the high abundances of total carbon (TC; sum of OC and EC), EC,

OC, SO_4^{2-}, NH_4^+, NO_3^-, and some trace elements indicative of lubrication oil additives (e.g., Mg, S, Ca, and Zn) and wear of vehicle, brake, or road surface (e.g., Al, Fe, and Cu) [55] were present at higher than 0.05% of $PM_{2.5}$ abundance. The $PM_{2.5}$ source profile for road dust is plotted in Figure 2c. The dust particles were enriched with OC, EC, and geological elements (e.g., Si, Ca, Fe, and Al). Some abundant elements could also originate from tire wear (e.g., Zn) and brake wear (e.g., Cu, Zn, Zr, Mo, and Sn) [20,56,57].

Figure 3 shows LPG, GV, and DV emission profiles resolved by PMF for CO_2, CO, NO_x, SO_2, and NMHC (normalized to the total measured NMHC mass concentrations). The most abundant NMHC species in the LPG profile were isobutane (23.2%), n-butane (23.0%), and propane (12.0%), indicating unburned LPG fuel. Guo et al. [54] found that these three species were the most abundant NMHCs from chassis dynamometer testing of LPG-fueled taxis at 70 km/h, with mass percentages of 16.0%, 19.4%, and 37.2% for isobutane, n-butane, and propane, respectively. The characteristic molar ratio of propane/(n-butane + isobutane) of LPG fuel vapor is 0.38 [53], while the measured propane/(n-butane + isobutane) ratio was 0.36 ± 0.07 in this tunnel study. The similar ratios between the LPG vapor and the tunnel samples indicate the contributions of evaporative losses from LPG vehicles to tunnel NMHCs. This observation contradicts the assumption that LPG vehicles do not have evaporative emissions in EMFAC-HK [27]. The gasoline profile contained the highest levels of aromatics, including toluene (22.8 wt%), m/p-xylene (6.6 wt%), and ethylbenzene (4.7 wt%). The high toluene level is likely related to its use as a gasoline additive to increase the octane index in Hong Kong [53]. High abundances of aromatic species were also found in gasoline vehicle exhaust in several previous studies [54,58]. The diesel profile shows more abundant ethene (14.4 wt%), ethyne (6.6 wt%), and ethane (7.1 wt%). Similar to the profile derived by Ling and Guo [59], the diesel profile also has high abundances of propane, isobutane, and n-butane, overlapping with the LPG profile. In addition, the diesel profile has the highest CO_2 and NO_x abundances among the three fuels.

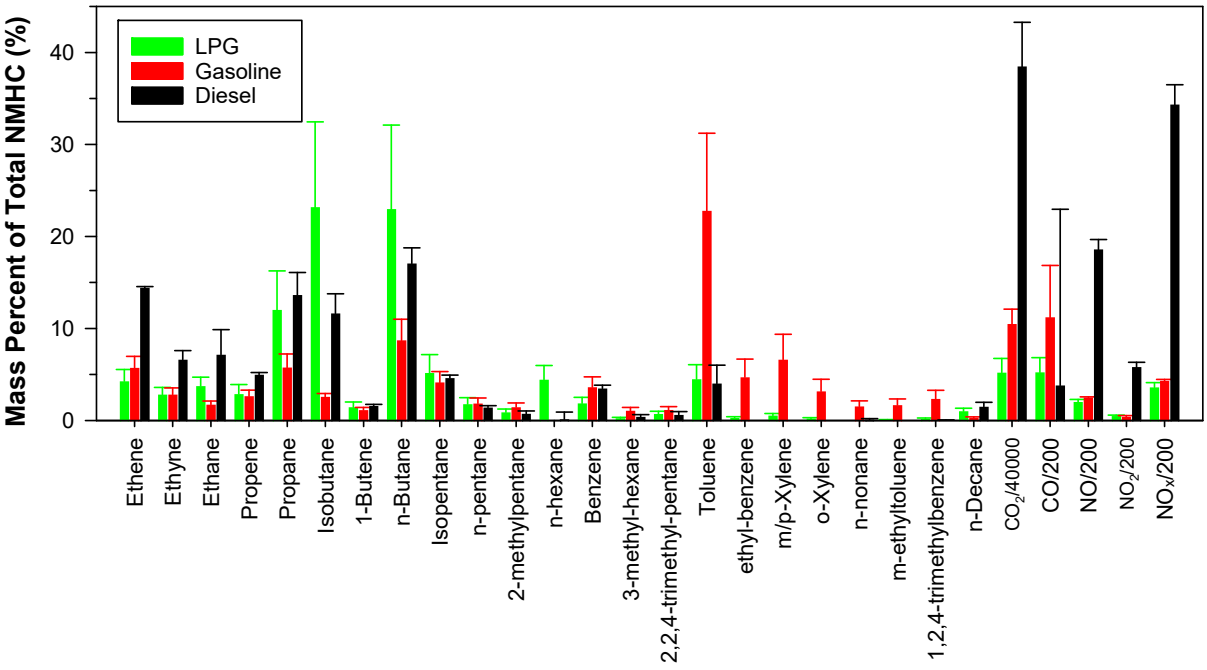

Figure 3. PMF-derived gas and NMHC factors associated with LPG, gasoline, and diesel vehicles. Only species with abundances >1% of total measured NMHC mass are shown for clarity. Error bars indicate the standard deviation from 10 replicate model runs.

The PMF-derived $PM_{2.5}$ source profiles for gasoline, LPG, and diesel emission are compared in Figure S7. The LPG profile has an EC/OC ratio of zero, in comparison with 0.36 and 2.9 for the gasoline and diesel profiles. The LPG profile has overall higher

abundances of particulate n-alkane/alkene, PAHs, hopane, and sterane. Due to the fact that LPG is a relatively simple mixture of hydrocarbon components with superior vaporizing characteristics, less PM is emitted from the fuel combustion process as compared to DV and GV [60]. Therefore, a larger fraction of LPG PM originates from lubrication oil, which is known to produce hopanes, steranes, and high-molecular-weight organics [61]. However, these differences could also be caused by uncertainties in the PMF apportionment. To our knowledge, no studies have reported detailed chemical compositions of $PM_{2.5}$ from directly measured LPG vehicle tailpipe emissions; such studies are warranted in the future to validate the $PM_{2.5}$ source profile for LPG vehicle emissions. Indeno[1,2,3-cd]pyrene and benzo[ghi]perylene were identified as markers for gasoline exhausts by Chow et al. [62]. However, they have relatively higher abundances in the LPG profile, indicating that these species may not be as useful gasoline markers when the traffic has a substantial LPG vehicle fraction. On the other hand, some heavier PAHs such as retene, benzo(ghi)fluoranthene, and methylfluoranthene were found to be most enriched in the gasoline profile. The diesel profile features much higher EC abundances (64%) compared to gasoline (21%) and LPG (0%).

Figure 4 compares the relative contributions of LPG, gasoline, and diesel vehicles to gaseous and $PM_{2.5}$ emissions from the vehicle fleet as estimated by PMF and EMFAC-HK, showing reasonable agreement. DV has the largest contribution to CO_2 (~65%), NO (77–80%), NO_2 (83–98%), NO_x (78–83%), SO_2 (66%; only available from PMF), and $PM_{2.5}$ (78–96%). It is expected that conventional DV has higher NO_x and $PM_{2.5}$ emissions than LPG and GV, and technological breakthroughs are needed to reduce NO_x and PM at the same time [63]. The higher CO_2 and SO_2 contributions are related to the higher EFs and lower fuel economy of DV [27]. DV contributions via PMF and EMFAC-HK estimates agree within 15% for most pollutants, with CO_2, NMHC, NO, and NO_x differing less than 3%. EMFAC-HK showed 18% higher DV contribution to $PM_{2.5}$, partially because EMFAC-HK assumes that LPG does not emit $PM_{2.5}$, whereas PMF attributed 7.4% $PM_{2.5}$ from LPG vehicles.

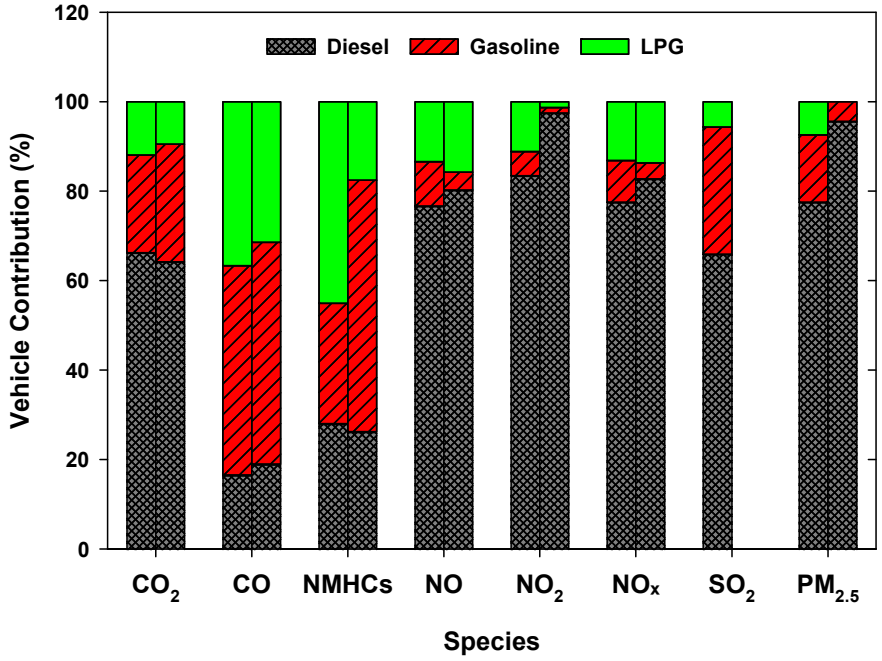

Figure 4. Relative source contribution estimates for LPG, gasoline, and diesel vehicle emissions as fractions of total vehicle emissions estimated by PMF (left bars) and EMFAC-HK (right bars).

Both GV and LPG have high contributions to CO and source attributions by PMF and EMFAC-HK differed less than 15%. These two methods also apportion similar CO_2 contributions by GV and LPG. However, larger differences are found for other pollutants.

Most of these species have the largest contributions from DV and the differences in DV contributions by PMF and EMFAC-HK led to discrepancies in LPG and GV apportionments. The EMFAC-HK attributed a much larger contribution of NMHCs by GV (56%) than LPG (18%), which is likely due to its unrealistic assumption that LPG and DV do not have any evaporative losses of NMHC.

Figure 5 shows PMF-derived source contribution estimates for $PM_{2.5}$ concentrations in the tunnel. In addition to vehicle emissions, secondary inorganic aerosols and road dust are included. DV emissions account for over 50% of tunnel $PM_{2.5}$ mass concentrations, followed by secondary sulfate (~20%). Road dust (including resuspended dust as well as brake, tire, and road surface wear) contributes to ~7% of $PM_{2.5}$ mass. Although not measured, the road dust contribution to the PM_{10} mass is expected to be higher due to larger-sized particles. Chemical composition analysis of $PM_{2.5}$ collected in the SMT shows that geological mineral abundances increased from 2% in 2003 to 5% in 2015, indicating that non-tailpipe emissions are becoming more important as tailpipe emissions decrease [28,64].

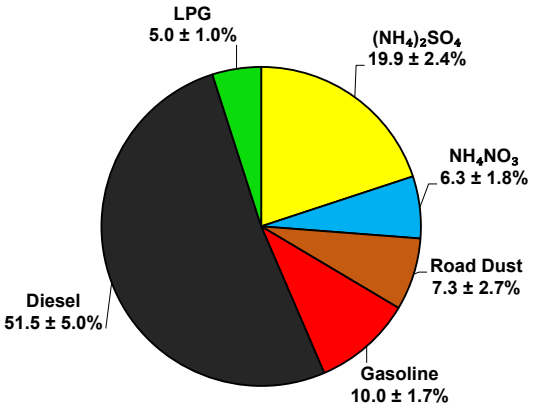

Figure 5. Average PMF-derived source contributions to $PM_{2.5}$ in the tunnel.

4. Conclusions

Estimations of EFs for different vehicle fleet compositions and their contributions to roadside air pollutant concentrations are valuable for emission control and air quality management policies. Due to the fact that all conventional vehicle tailpipe emissions originate from the internal combustion of hydrocarbon fuels, most combustion products are similar, making the separation of emissions by different vehicle types challenging. Tunnel studies have been used to determine real-world on-road vehicle emissions, and EFs by different vehicle types are estimated by linear regression, receptor-based source apportionment, or emission models. However, the accuracy and uncertainties of these methods have not been sufficiently discussed. This study applied SLR, MLR, PMF, and EMFAC-HK to estimate the EFs of LPG, GV, and DV measured in the SMT in Hong Kong to compare the performance of these methods. The key findings of this study are:

1. Increasing the time resolution of the pollutant concentration and fleet composition data significantly reduces EF uncertainties by linear regressions. By increasing the time resolution from 2 h to 15 min, the relative uncertainties of the NO_x EFs reduced from 79% to 33% for NDV and from 32% to 14% for DV. The increased time resolution not only increases the number of data points in the regression, but also enhances the differentiation of emissions among different vehicle types. The time resolution is determined by the data intervals of gas and particle sampling as well as that of traffic categorization. It is also influenced by traffic volume as too high time resolution will likely increase traffic-counting statistical errors. The optimum time resolution needs to be determined from sensitivity tests at several time resolutions for each study.
2. While SLR is the simplest among the four apportionment methods, caution should be taken when using SLR with very narrow traffic composition ranges, as the uncertainties of EFs by extrapolating the regression to f_{DV} of 0% and 100% can be excessively

large. Efforts should be made to increase the fleet composition's variability, such as measuring in tunnels with separated LD and HD traffic or by measuring different periods with a variety of fleet mixes.

3. With respect to the four EF calculation methods, MLR has the highest relative uncertainties, with many values exceeding ±100%, causing LPG and NDV EFs for many pollutants not statistically different from zero. Compared to SLR, MLR may resolve EFs for more than two vehicle categories, but EFs uncertainties by MLR were typically over twice those by SLR. EMFAC-HK has the lowest (<2%) relative uncertainties, due to its assignment of a single average EF value for each category under specific environmental and operating conditions. The relative uncertainties of SLR and PMF are comparable for many EFs by DV and NDV.
4. Among the apportionment methods compared in this study, PMF is likely the most reliable and useful, as it simultaneously seeks the source signatures and source contributions by minimizing the deviation between modeled and measured concentrations. In addition to contributions from different vehicle categories, it also identifies contributions from other sources. In SMT, diesel, gasoline, and LPG vehicle emissions account for 52%, 10%, and 5% of $PM_{2.5}$ concentrations, while ammonium sulfate (~20%), ammonium nitrate (6%), and road dust (7%) are also large contributors. Additionally, PMF produces source profiles indicating key signature chemical composition for each source.
5. PMF and EMFAC-HK agree reasonably well for the relative contributions of LPG, gasoline, and diesel vehicles to gases and $PM_{2.5}$ emissions by the vehicle fleet in the SMT. DV makes the largest contribution to CO_2, NO_x, and $PM_{2.5}$, while GV makes the largest contribution to CO. Comparing source- and receptor-oriented models is recommended in source apportionment studies to reveal and resolve potential errors in the models and to reduce modeling uncertainties.
6. The LPG gas source profile shows abundant isobutane, n-butane, and propane, indicating unburned LPG fuel; the LPG $PM_{2.5}$ source profile has a higher abundance of organic molecules but nearly zero EC. The GV gas profile contains the highest levels of aromatics, including toluene, m/p-xylene, and ethylbenzene; the GV $PM_{2.5}$ source profile shows higher abundances of heavier PAHs such as retene, benzo(ghi)fluoranthene, and methylfluoranthene. The DV gas profile has the highest CO_2 and NO_x abundances, and the DV $PM_{2.5}$ source profile shows the highest EC abundance. Due to continuous changes in fuels, combustion technologies, and emission controls, the vehicle source profiles vary with location and time and need to be continuously evaluated and updated.
7. Several knowledge gaps remain. The EMFAC-HK assumes zero tailpipe PM emissions from LPG vehicles, which may not be true as lubrication oil generates particles. To our best knowledge, there have not been direct tailpipe emission measurements from LPG vehicles; these measurements are needed to accurately determine EFs and source profiles of PM from LPG vehicles. The EMFAC-HK also assumes that LPG and DV do not have evaporative NMHC emissions, which does not agree with the abundant LPG fuel molecules observed in this study. In the interest of further reducing ozone and secondary organic aerosol pollutions, future studies should quantify the evaporative emission contributions for both LPG and DV and include these in emission models.
8. As the true emissions by different fleet compositions are not known, the apportionment accuracy cannot be assessed by comparing with true values. A "weight of evidence" approach using additional available information (e.g., local emission inventories, source profiles, and modeling performance measures), running multiple receptor-modeling techniques, or reconciling receptor-oriented and source-oriented models can increase the degree of confidence.

Supplementary Materials: Supplemental tables and figures can be downloaded at: https://www.mdpi.com/article/10.3390/atmos13071066/s1. Figure S1. Schematic diagram of: (a) sampling configuration in the east section of the Shing Mun Tunnel (SMT) and (b) sampling setup at the outlet site of the SMT in 2015; Figure S2. The fraction of the Q value change as the number of factors increases from m to m + 1 in the PMF modeling. Q value change stabilizes after m = 6, indicating that a 6-factor solution is appropriate for this dataset; Figure S3. PMF fitting performance by $PM_{2.5}$ components, as indicated by the scaled residual vs. correlation between measured and modeled concentrations. Key $PM_{2.5}$ species are labeled; Figure S4. PMF fitting performance by gas species, as indicated by the scaled residual vs. correlation between measured and modeled NMHC concentrations. Key species are labeled; Figure S5. Linear regression of pollutant emission factors vs. diesel vehicle fractions. The red solid line shows robust regression excluding the outlier (unfilled symbols) data points. The blue dashed lines indicate the 95% coincidence intervals for the robust regression; Figure S6. Comparison of emission factors for fleet components by different methods. Error bars represent the 95% confidence intervals of the mean. Figure S7. PMF-derived $PM_{2.5}$ factors associated with diesel, LPG, and gasoline vehicles (left panel: ions, carbon, elements, and PAHs; right panel: alkanes, alkenes, hopanes, and steranes). Only species with abundances >0.01% of measured $PM_{2.5}$ mass are shown for clarity. Error bars indicate variability (standard deviation) from 10 replicate model runs. Table S1. Emission factors (EF_D; average $\pm$ 95% confidence interval) by simple linear regression (SLR) and multiple linear regression (MLR). Data with a red font indicate that the estimates are not statistically significant. Table S2. Relative uncertainties (expanded uncertainty/average) of emission factors by different methods. Data with an italic purple font indicate that the absolute relative uncertainty exceeds 100%. Table S3. Statistical significance (p-values) of differences between emission factors obtained by different methods. Green font indicates $p \geq 0.05$.

Author Contributions: Conceptualization, X.W., K.-F.H., S.-C.L., J.G.W. and J.C.C.; methodology, X.W., L.-W.A.C. and M.L.; software, L.-W.A.C. and M.L.; validation, X.W., L.-W.A.C. and M.L.; formal analysis, X.W., L.-W.A.C. and M.L.; resources, X.W. and S.-C.L.; data curation, X.W., K.-F.H. and S.S.H.H.; writing—original draft preparation, X.W.; writing—review and editing, L.-W.A.C., M.L., K.-F.H., S.-C.L., S.S.H.H., J.C.C. and J.G.W.; visualization, X.W., L.-W.A.C. and M.L.; project administration, X.W. and K.-F.H.; funding acquisition, X.W. and S.-C.L. All authors have read and agreed to the published version of the manuscript.

Funding: This study was jointly supported by HEI Research Agreement Number 4947-RFPA14-1/15-1, the Research Grants Council of Hong Kong Government (Project No. T24/504/17), and the National Key Research and Development Program of China (2016YFA0203000).

Institutional Review Board Statement: Not applicable.

Informed Consent Statement: Not applicable.

Data Availability Statement: The data presented in this study are openly available in the Harvard Dataverse [65]. Data for figures and tables are available on request from the corresponding author.

Conflicts of Interest: The authors declare no conflict of interest.

References

1. Smit, R.; Ntziachristos, L.; Boulter, P. Validation of road vehicle and traffic emission models—A review and meta-analysis. *Atmos. Environ.* **2010**, *44*, 2943–2953. [CrossRef]
2. Franco, V.; Kousoulidou, M.; Muntean, M.; Ntziachristos, L.; Hausberger, S.; Dilara, P. Road vehicle emission factors development: A review. *Atmos. Environ.* **2013**, *70*, 84–97. [CrossRef]
3. HEI. *Traffic-Related Air Pollution: A Critical Review of the Literature on Emissions, Exposure, and Health Effects*; HEI Special Report 17; Health Effects Institute Panel on the Health Effects of Traffic-Related Air Pollution: Boston, MA, USA, 2010; Available online: http://pubs.healtheffects.org/getfile.php?u=553 (accessed on 5 August 2014).
4. El-Fadel, M.; Hashisho, Z. Vehicular Emissions in Roadway Tunnels: A Critical Review. *Crit. Rev. Environ. Sci. Technol.* **2001**, *31*, 125–174. [CrossRef]
5. Marinello, S.; Lolli, F.; Gamberini, R. Roadway tunnels: A critical review of air pollutant concentrations and vehicular emissions. *Transp. Res. Part D Transp. Environ.* **2020**, *86*, 102478. [CrossRef]
6. Pierson, W.R.; Gertler, A.W.; Robinson, N.F.; Sagebiel, J.C.; Zielinska, B.; Bishop, G.A.; Stedman, D.H.; Zweidinger, R.B.; Ray, W.D. Real-world automotive emissions—Summary of studies in the Fort McHenry and Tuscarora mountain tunnels. *Atmos. Environ.* **1996**, *30*, 2233–2256. [CrossRef]

7. Colberg, C.A.; Tona, B.; Catone, G.; Sangiorgio, C.; Stahel, W.A.; Sturm, P.; Staehelin, J. Statistical analysis of the vehicle pollutant emissions derived from several European road tunnel studies. *Atmos. Environ.* **2005**, *39*, 2499–2511. [CrossRef]
8. Smit, R.; Kingston, P.; Wainwright, D.H.; Tooker, R. A tunnel study to validate motor vehicle emission prediction software in Australia. *Atmos. Environ.* **2017**, *151*, 188–199. [CrossRef]
9. Song, C.; Ma, C.; Zhang, Y.; Wang, T.; Wu, L.; Wang, P.; Liu, Y.; Li, Q.; Zhang, J.; Dai, Q.; et al. Heavy-duty diesel vehicles dominate vehicle emissions in a tunnel study in northern China. *Sci. Total Environ.* **2018**, *637–638*, 431–442. [CrossRef]
10. Watson, J.G.; Chow, J.C.; Engling, G.; Chen, L.-W.A.; Wang, X.L. Source apportionment: Principles and methods. In *Airborne Particulate Matter: Sources, Atmospheric Processes and Health*; Harrison, R.M., Ed.; Royal Society of Chemistry: London, UK, 2016; pp. 72–125.
11. Watson, J.G.; Cooper, J.A.; Huntzicker, J.J. The effective variance weighting for least squares calculations applied to the mass balance receptor model. *Atmos. Environ.* **1984**, *18*, 1347–1355. [CrossRef]
12. Thurston, G.D.; Spengler, J.D. A quantitative assessment of source contributions to inhalable particulate matter pollution in metropolitan Boston. *Atmos. Environ.* **1985**, *19*, 9–25. [CrossRef]
13. Paatero, P.; Tapper, U. Positive matrix factorization: A non-negative factor model with optimal utilization of error estimates of data values. *Environmetrics* **1994**, *5*, 111–126. [CrossRef]
14. Taiwo, A.M.; Harrison, R.M.; Shi, Z. A review of receptor modelling of industrially emitted particulate matter. *Atmos. Environ.* **2014**, *97*, 109–120. [CrossRef]
15. Watson, J.G.; Zhu, T.; Chow, J.C.; Engelbrecht, J.P.; Fujita, E.M.; Wilson, W.E. Receptor modeling application framework for particle source apportionment. *Chemosphere* **2002**, *49*, 1093–1136. [CrossRef]
16. HEI. *The Future of Vehicle Fuels and Technologies: Anticipating Health Benefits and Challenges*; HEI Communication 16; Health Effects Institute Special Committee on Emerging Technologies: Boston, MA, USA, 2011; Available online: http://pubs.healtheffects.org/getfile.php?u=635 (accessed on 5 August 2014).
17. Fraser, M.P.; Buzcu, B.; Yue, Z.W.; McGaughey, G.R.; Desai, N.R.; Allen, D.T.; Seila, R.L.; Lonneman, W.A.; Harley, R.A. Separation of Fine Particulate Matter Emitted from Gasoline and Diesel Vehicles Using Chemical Mass Balancing Techniques. *Environ. Sci. Technol.* **2003**, *37*, 3904–3909. [CrossRef]
18. Chow, J.C.; Watson, J.G. Review of PM2.5 and PM10 Apportionment for Fossil Fuel Combustion and Other Sources by the Chemical Mass Balance Receptor Model. *Energy Fuels* **2002**, *16*, 222–260. [CrossRef]
19. Fujita, E.M.; Campbell, D.E.; Arnott, W.P.; Chow, J.C.; Zielinska, B. Evaluations of the Chemical Mass Balance Method for Determining Contributions of Gasoline and Diesel Exhaust to Ambient Carbonaceous Aerosols. *J. Air Waste Manag. Assoc.* **2007**, *57*, 721–740. [CrossRef]
20. Pant, P.; Harrison, R.M. Estimation of the contribution of road traffic emissions to particulate matter concentrations from field measurements: A review. *Atmos. Environ.* **2013**, *77*, 78–97. [CrossRef]
21. Pant, P.; Harrison, R.M. Critical review of receptor modelling for particulate matter: A case study of India. *Atmos. Environ.* **2012**, *49*, 1–12. [CrossRef]
22. Liu, Y.; Wang, S.; Lohmann, R.; Yu, N.; Zhang, C.; Gao, Y.; Zhao, J.; Ma, L. Source apportionment of gaseous and particulate PAHs from traffic emission using tunnel measurements in Shanghai, China. *Atmos. Environ.* **2015**, *107*, 129–136. [CrossRef]
23. Lawrence, S.; Sokhi, R.; Ravindra, K.; Mao, H.; Prain, H.D.; Bull, I.D. Source apportionment of traffic emissions of particulate matter using tunnel measurements. *Atmos. Environ.* **2013**, *77*, 548–557. [CrossRef]
24. Chen, L.-W.A.; Watson, J.G.; Chow, J.C.; DuBois, D.W.; Herschberger, L. PM2.5 Source Apportionment: Reconciling Receptor Models for U.S. Nonurban and Urban Long-Term Networks. *J. Air Waste Manag. Assoc.* **2011**, *61*, 1204–1217. [CrossRef] [PubMed]
25. NRC. *Modeling Mobile-Source Emissions*; Transportation Research Board, National Research Council, The National Academies Press: Washington, DC, USA, 2000; 258p.
26. Fujita, E.M.; Campbell, D.E.; Zielinska, B.; Chow, J.C.; Lindhjem, C.E.; DenBleyker, A.; Bishop, G.A.; Schuchmann, B.G.; Stedman, D.H.; Lawson, D.R. Comparison of the MOVES2010a, MOBILE6.2 and EMFAC2007 mobile source emissions models with on-road traffic tunnel and remote sensing measurements. *J. Air Waste Manag. Assoc.* **2012**, *62*, 1134–1149. [CrossRef] [PubMed]
27. Wang, X.L.; Chen, L.-W.A.; Ho, K.-F.; Chan, C.S.; Zhang, Z.; Lee, S.-C.; Chow, J.C.; Watson, J.G. Comparison of Vehicle Emissions by EMFAC-HK Model and Tunnel Measurement in Hong Kong. *Atmos. Environ.* **2021**, *256*, 118452. [CrossRef]
28. Wang, X.L.; Ho, K.-F.; Chow, J.C.; Kohl, S.D.; Chan, C.S.; Cui, L.; Lee, S.-c.F.; Chen, L.-W.A.; Ho, S.S.H.; Cheng, Y.; et al. Hong Kong vehicle emission changes from 2003 to 2015 in the Shing Mun Tunnel. *Aerosol Sci. Technol.* **2018**, *52*, 1085–1098. [CrossRef]
29. Wang, X.L.; Khlystov, A.; Ho, K.F.; Campbell, D.; Chow, J.C.; Kohl, S.D.; Watson, J.G.; Lee, S.C.; Chen, L.-W.A.; Lu, M.; et al. *Real-World Vehicle Emissions Characterization for the Shing Mun Tunnel in Hong Kong and Fort McHenry Tunnel in the United States*; Health Effects Institute: Boston, MA, USA, 2019. Available online: https://www.healtheffects.org/system/files/WangRR199.pdf (accessed on 10 December 2021).
30. Cui, L.; Wang, X.L.; Ho, K.F.; Gao, Y.; Liu, C.; Ho, S.S.; Li, H.; Lee, S.C.; Wang, X.; Jiang, B.; et al. Decrease of VOC emissions from vehicular emissions in Hong Kong from 2003 to 2015: Results from a tunnel study. *Atmos. Environ.* **2018**, *177*, 64–74. [CrossRef]
31. U.S. EPA. *Compendium Method TO-15: Determination of Volatile Organic Compounds (VOCs) in Air Collected in Specially-Prepared Canisters and Analyzed by Gas Chromatography/Mass Spectrometry (GC/MS)*; U.S. Environmental Protection Agency: Research Triangle Park, NC, USA, 1999.

32. Watson, J.G.; Tropp, R.J.; Kohl, S.D.; Wang, X.L.; Chow, J.C. Filter processing and gravimetric analysis for suspended particulate matter samples. *Aerosol Sci. Eng.* **2017**, *1*, 193–205. [CrossRef]
33. Watson, J.G.; Chow, J.C.; Frazier, C.A. X-ray fluorescence analysis of ambient air samples. In *Elemental Analysis of Airborne Particles*; Landsberger, S., Creatchman, M., Eds.; Gordon and Breach Science: Amsterdam, The Netherlands, 1999; Volume 1, pp. 67–96.
34. Chow, J.C.; Watson, J.G. Enhanced ion chromatographic speciation of water-soluble $PM_{2.5}$ to improve aerosol source apportionment. *Aerosol Sci. Eng.* **2017**, *1*, 7–24. [CrossRef]
35. Chow, J.C.; Watson, J.G.; Chen, L.-W.A.; Chang, M.C.O.; Robinson, N.F.; Trimble, D.; Kohl, S. The IMPROVE_A temperature protocol for thermal/optical carbon analysis: Maintaining consistency with a long-term database. *J. Air Waste Manag. Assoc.* **2007**, *57*, 1014–1023. [CrossRef]
36. Chow, J.C.; Yu, J.Z.; Watson, J.G.; Ho, S.S.H.; Bohannan, T.L.; Hays, M.D.; Fung, K.K. The application of thermal methods for determining chemical composition of carbonaceous aerosols: A review. *J. Environ. Sci. Health Part A-Toxic/Hazard. Subst. Environ. Eng.* **2007**, *42*, 1521–1541. [CrossRef] [PubMed]
37. Ho, S.S.H.; Yu, J.Z.; Chow, J.C.; Zielinska, B.; Watson, J.G.; Sit, E.H.L.; Schauer, J.J. Evaluation of an in-injection port thermal desorption-gas chromatography/mass spectrometry method for analysis of non-polar organic compounds in ambient aerosol samples. *J. Chromatogr. A* **2008**, *1200*, 217–227. [CrossRef]
38. Ho, S.S.H.; Yu, J.Z. In-injection port thermal desorption and subsequent gas chromatography-mass spectrometric analysis of polycyclic aromatic hydrocarbons and n-alkanes in atmospheric aerosol samples. *J. Chromatogr. A* **2004**, *1059*, 121–129. [CrossRef] [PubMed]
39. Chow, J.C.; Watson, J.G.; Chen, L.-W.A.; Rice, J.; Frank, N.H. Quantification of $PM_{2.5}$ organic carbon sampling artifacts in US networks. *Atmos. Chem. Phys.* **2010**, *10*, 5223–5239. [CrossRef]
40. Gertler, A.W.; Gillies, J.A.; Pierson, W.R.; Rogers, C.F.; Sagebiel, J.C.; Abu-Allaban, M.; Coulombe, W.; Tarnay, L.; Cahill, T.A. *Real-World Particulate Matter and Gaseous Emissions from Motor Vehicles in a Highway Tunnel-HEI Research Report Number 107*; Health Effects Institute: Boston, MA, USA, 2002; Available online: http://pubs.healtheffects.org/getfile.php?u=171 (accessed on 10 October 2014).
41. Leys, C.; Ley, C.; Klein, O.; Bernard, P.; Licata, L. Detecting outliers: Do not use standard deviation around the mean, use absolute deviation around the median. *J. Exp. Soc. Psychol.* **2013**, *49*, 764–766. [CrossRef]
42. Chen, L.-W.A.; Lowenthal, D.H.; Watson, J.G.; Koracin, D.; Kumar, N.; Knipping, E.M.; Wheeler, N.; Craig, K.; Reid, S. Toward Effective Source Apportionment Using Positive Matrix Factorization: Experiments with Simulated PM2.5 Data. *J. Air Waste Manag. Assoc.* **2010**, *60*, 43–54. [CrossRef]
43. Reff, A.; Eberly, S.I.; Bhave, P.V. Receptor modeling of ambient particulate matter data using positive matrix factorization: Review of existing methods. *J. Air Waste Manag. Assoc.* **2007**, *57*, 146–154. [CrossRef]
44. Cheng, Y.; Lee, S.C.; Ho, K.F.; Louie, P.K.K. On-road particulate matter ($PM_{2.5}$) and gaseous emissions in the Shing Mun Tunnel, Hong Kong. *Atmos. Environ.* **2006**, *40*, 4235–4245. [CrossRef]
45. Watson, J.G.; Chow, J.C.; Lu, Z.; Fujita, E.M.; Lowenthal, D.H.; Lawson, D.R. Chemical mass balance source apportionment of PM_{10} during the Southern California Air Quality Study. *Aerosol Sci. Technol.* **1994**, *21*, 1–36. [CrossRef]
46. Chen, L.-W.A.; Watson, J.G.; Chow, J.C.; Green, M.C.; Inouye, D.; Dick, K. Wintertime particulate pollution episodes in an urban valley of the western U.S.: A case study. *Atmos. Chem. Phys.* **2012**, *12*, 10051–10064.
47. Chen, L.-W.A.; Cao, J. PM2.5 Source Apportionment Using a Hybrid Environmental Receptor Model. *Environ. Sci. Technol.* **2018**, *52*, 6357–6369. [CrossRef]
48. Chen, L.-W.A.; Chow, J.C.; Wang, X.; Cao, J.; Mao, J.; Watson, J.G. Brownness of Organic Aerosol over the United States: Evidence for Seasonal Biomass Burning and Photobleaching Effects. *Environ. Sci. Technol.* **2021**, *55*, 8561–8572. [CrossRef]
49. Tian, J.; Wang, Q.; Han, Y.; Ye, J.; Wang, P.; Pongpiachan, S.; Ni, H.; Zhou, Y.; Wang, M.; Zhao, Y.; et al. Contributions of aerosol composition and sources to particulate optical properties in a southern coastal city of China. *Atmos. Res.* **2020**, *235*, 104744. [CrossRef]
50. Stout, S.A.; Liu, B.; Millner, G.C.; Hamlin, D.; Healey, E. Use of chemical fingerprinting to establish the presence of spilled crude oil in a residential area following hurricane Katrina, St. Bernard parish, Louisiana. *Environ. Sci. Technol.* **2007**, *41*, 7242–7251. [CrossRef] [PubMed]
51. Ho, K.F.; Lee, S.C.; Ho, W.K.; Blake, D.R.; Cheng, Y.; Li, Y.S.; Ho, S.S.H.; Fung, K.; Louie, P.K.K.; Park, D. Vehicular emission of volatile organic compounds (VOCs) from a tunnel study in Hong Kong. *Atmos. Chem. Phys.* **2009**, *9*, 7491–7504. [CrossRef]
52. Paatero, P. Least squares formulation of robust non-negative factor analysis. *Chemom. Intell. Lab. Sys.* **1997**, *37*, 23–35. [CrossRef]
53. Tsai, W.Y.; Chan, L.Y.; Blake, D.R.; Chu, K.W. Vehicular fuel composition and atmospheric emissions in South China: Hong Kong, Macau, Guangzhou, and Zhuhai. *Atmos. Chem. Phys.* **2006**, *6*, 3281–3288. [CrossRef]
54. Guo, H.; Zou, S.C.; Tsai, W.Y.; Chan, L.Y.; Blake, D.R. Emission characteristics of nonmethane hydrocarbons from private cars and taxis at different driving speeds in Hong Kong. *Atmos. Environ.* **2011**, *45*, 2711–2721. [CrossRef]
55. Whitacre, S.D.; Tsai, H.-C.; Orban, J. *Lubricant Basestock and Additive Effects on Diesel Engine Emissions*; U.S. Departament of Energy: Washington, DC, USA, 2002. Available online: http://www.afdc.energy.gov/pdfs/32842,pdf (accessed on 27 December 2016).

56. Denier van der Gon, H.A.C.; Gerlofs-Nijland, M.E.; Gehrig, R.; Gustafsson, M.; Janssen, N.; Harrison, R.M.; Hulskotte, J.; Johansson, C.; Jozwicka, M.; Keuken, M.; et al. The Policy Relevance of Wear Emissions from Road Transport, Now and in the Future—An International Workshop Report and Consensus Statement. *J. Air Waste Manag. Assoc.* **2013**, *63*, 136–149. [CrossRef] [PubMed]
57. Gietl, J.K.; Lawrence, R.; Thorpe, A.J.; Harrison, R.M. Identification of brake wear particles and derivation of a quantitative tracer for brake dust at a major road. *Atmos. Environ.* **2010**, *44*, 141–146. [CrossRef]
58. Schauer, J.J.; Kleeman, M.J.; Cass, G.R.; Simoneit, B.R.T. Measurement of Emissions from Air Pollution Sources. 5. C1-C32 Organic Compounds from Gasoline-Powered Motor Vehicles. *Environ. Sci. Technol.* **2002**, *36*, 1169–1180. [CrossRef]
59. Ling, Z.H.; Guo, H. Contribution of VOC sources to photochemical ozone formation and its control policy implication in Hong Kong. *Environ. Sci. Policy* **2014**, *38*, 180–191. [CrossRef]
60. Myung, C.-L.; Ko, A.; Lim, Y.; Kim, S.; Lee, J.; Choi, K.; Park, S. Mobile source air toxic emissions from direct injection spark ignition gasoline and LPG passenger car under various in-use vehicle driving modes in Korea. *Fuel Process. Technol.* **2014**, *119*, 19–31. [CrossRef]
61. Fujita, E.M.; Zielinska, B.; Campbell, D.E.; Arnott, W.P.; Sagebiel, J.C.; Mazzoleni, L.; Chow, J.C.; Gabele, P.A.; Crews, W.; Snow, R. Variations in speciated emissions from spark-ignition and compression-ignition motor vehicles in California's south coast air basin. *J. Air Waste Manag. Assoc.* **2007**, *57*, 705. [CrossRef] [PubMed]
62. Chow, J.C.; Watson, J.G.; Lowenthal, D.H.; Chen, L.-W.A.; Zielinska, B.; Mazzoleni, L.R.; Magliano, K.L. Evaluation of organic markers for chemical mass balance source apportionment at the Fresno supersite. *Atmos. Chem. Phys.* **2007**, *7*, 1741–1754. [CrossRef]
63. Dec, J.E. Advanced compression-ignition engines—Understanding the in-cylinder processes. *Proc. Combust. Inst.* **2009**, *32*, 2727–2742. [CrossRef]
64. Amato, F.; Cassee, F.R.; Denier van der Gon, H.A.C.; Gehrig, R.; Gustafsson, M.; Hafner, W.; Harrison, R.M.; Jozwicka, M.; Kelly, F.J.; Moreno, T.; et al. Urban air quality: The challenge of traffic non-exhaust emissions. *J. Hazard. Mater.* **2014**, *275*, 31–36. [CrossRef] [PubMed]
65. Shing Mun Tunnel and Fort McHenry Tunnel. Available online: https://dataverse.harvard.edu/dataverse/tunnels2019 (accessed on 1 June 2022).